

## Network of Ordered Phases in PE-PEE Diblock Copolymers

Hiroshi Takenouchi<sup>1</sup>, Damian A Hajduk<sup>2</sup> and Frank S. Bates

[1] Kawasaki Development Center, Montell SDK Sunrise Ltd.,2-3-2, Yako, Kawasaki-ku, Kawasaki, Japan.

[2] Symyx Technologies, 3100 Central Expressway, Sunnydale, California 95951

[3] Department of Chemical Engineering and Materials Science, University of Minnesota, Minneapolis MN 55455

*The phase behavior and network of order-order phase transitions occurring in binary mixtures of poly(ethylene)-poly(ethylene)(PE-PEE) diblock copolymers containing between 60 and 75% by volume PE have been characterized near the order-disorder transition (ODT) by dynamic mechanical spectroscopy (DMS) and small-angle X-ray scattering (SAXS). Three equilibrium phases (lamellae - L, gyroid - G, and cylinders - C) and one metastable phase (perforated layers - PL) are identified in a phase portrait defined by the composition  $\langle f_{PE} \rangle$  and combination parameter  $\chi \langle N \rangle$  where  $\chi$  and  $\langle N \rangle$  are the segment-segment interaction parameter and average degree of polymerization. These results unify disparate past findings on the complex phase behavior of diblock copolymer melts near the ODT.*

### Introduction

Although the phenomenon of microphase separation in block copolymers has been studied for over three decades, a detailed appreciation of phase behavior in the intermediate and weak segregation limits was not established until the past decade. In fact, the first report of an order-order phase transition (OOT) in a block copolymer melt occurred just 8 years ago [1], followed soon thereafter by many other examples that resulted in the identification of several relatively complete phase diagrams [2-5]. Five morphologies have been established for diblock melts: spheres (S) packed on a body centered cubic lattice; cylinders (C) arranged on a hexagonal lattice; the gyroid (G), a triply periodic and tricontinuous structure with  $Ia3d$  space group symmetry; lamellae (L), a smectic morphology; perforated layers (PL), a layered structure that contains a hexagonal arrangement of

passages through one of the layered microdomain spaces. Figure 1 illustrates these structures. A combination of experiment [6] and theory [7] has established with fair certainty that the PL phase is metastable, while the other structures occur at equilibrium.

Near the order-disorder transition (ODT), phase transitions between ordered phases can be realized at certain polymer compositions by changing temperature (or pressure). These OOT's generally are accompanied by significant changes in the viscoelastic properties of the material, thereby providing a convenient mechanical signal for establishing  $T_{OOT}$ ; this method of locating phase transitions in block copolymers has been employed to find  $T_{ODT}$ 's for many years [8-11]. Subsequently, the domain type and packing symmetry can be ascertained using small angle X-ray and/or neutron scattering (SAXS and SANS), and electron microscopy. Along with establishing static phase behavior we have employed this approach in exploring the underlying OOT mechanisms and kinetic pathways dictated by epitaxial relationships [12].

Earlier work on nearly monodisperse poly(ethylene)-poly(ethylene)(PE-PEE) diblock copolymers with  $0.25 \leq f_{PE} \leq 0.5$  ( $f_{PE}$  is the volume fraction of PE), and blends of  $f_{PE} = 0.37$  and  $0.46$  copolymers, established the viability of using binary mixtures of diblocks to determine phase behaviour near the ODT as a function of the average composition  $\langle f_{PE} \rangle$  [3]. Using just two diblocks the composition can be varied continuously, avoiding the need to synthesize separate macromolecules, a time consuming and tedious process. This prior investigation, along with several related ones, established that transformations between ordered phases are often kinetically limited, leading to substantial hysteresis on heating and cooling, in some circumstances generating long-lived metastable states. Recently, we have concluded that the PL morphology is such a metastable phase [6], appearing as a transient state during the transformation of lamellae to the gyroid structure. Theoretical calculations [7,13-15] support this finding and provide a rationale for the long-lived nature of the PL phase. In general, the morphological pathway followed upon heating or cooling a block copolymer melt is governed by at least two factors: epitaxial relationships and the rate of heating or cooling.

Sample	<sup>a</sup> f <sub>PE</sub>	<sup>b,c</sup> M <sub>n</sub> (kg mol <sup>-1</sup> )	<sup>b</sup> M <sub>w</sub> /M <sub>n</sub>	<sup>d</sup> phases (°C)
PE-PEE-7	0.75	44	1.05	C-(148)-Dis
PE-PEE-6	0.65	43	1.05	L-(143)-PL-(166)-G-(197)-C-(202)-Dis
PE-PEE-17	0.60	42	1.05	L-(242)-D

- Volume fraction of PE based on NMR analysis, synthesis stoichiometry, and published densities [21].
- Determined from GPC analysis.
- From synthesis stoichiometry.
- Determined by DMS (while heating at 0.3 °C/min) and SAXS.

**Table 1.** Block Copolymer Molecular Characteristics

The work reported here compliments our previous study with PE-PEE blends [3], covering the composition range  $0.60 \leq \langle f_{PE} \rangle \leq 0.75$ , where the L, PL, G, and C phases are all found. Dynamic mechanical spectroscopy (DMS) and SAXS experiments have been used to determine the phase behaviour as a function of  $\langle f_{PE} \rangle$  and temperature. By varying the rate of heating and cooling through order-order transitions we have gained fresh insights regarding phase transition dynamics, and completed our picture of the kinetic pathways between the L, PL, G, and C morphologies.

## Experimental

The PE-PEE diblock copolymers used in this study were synthesized and characterized using well-established procedures [16, 17]. Molecular characteristics are listed in Table 1. These saturated hydrocarbon polymers are stable against oxidative degradation. The PE block is semicrystalline with a melting temperature of  $T_m \approx 108$  °C while the PEE block exhibits a glass transition temperature at about -20 °C. All measurements reported here were conducted in the melt state.

Blends of PE-PEE-7 and PE-PEE-17 were prepared by codissolution in toluene at 90 °C followed by precipitation in methanol and vacuum drying at 140 °C for 12 hours.

DMS measurements were performed on a Rheometrics RSAII solids analyzer with a shear sandwich fixture containing a 0.5 mm gap. A nitrogen gas purge was used to minimize sample oxidation at high temperatures. The work reported here was based on a single type of measurement: heating or cooling at a fixed rate (0.1 - 2.0 °C/min)

while measuring the linear dynamic elastic shear modulus  $G'(T)$  at a fixed frequency of 0.5 rad/s. Transmission electron microscope (TEM) images were obtained from selected samples. Although not presented here, the TEM results were consistent with the phase assignments identified in the following sections.

Small-angle X-ray scattering (SAXS) patterns were obtained on a beamline at the University of Minnesota; a description of this instrument is given elsewhere [6]. SAXS patterns were used as the principal tool for identifying phase symmetry and

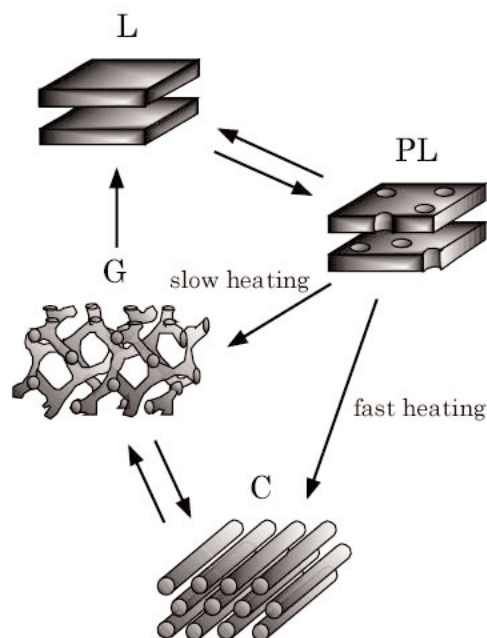


**Figure 1:** Ordered morphologies documented in diblock copolymers near the order-disorder transition: L-lamellae, PL-perforated layers, G-gyroid, C-cylinders. The L, G, C structures constitute equilibrium phases while PL is a metastable state. Arrows identify documented order-order transitions (OOT's).

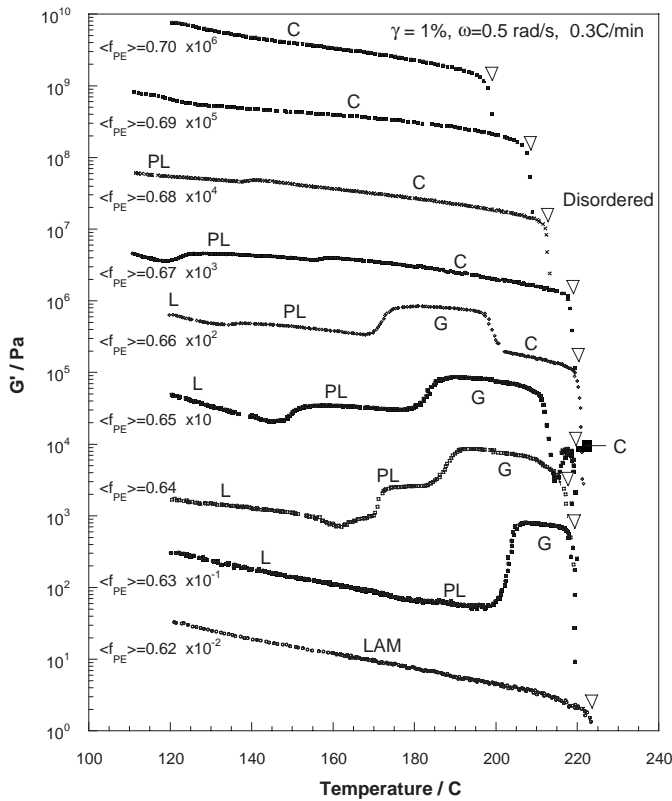


**Figure 2:** Linear dynamic elastic shear modulus ( $G'$ ) as a function of temperature for mixtures of PE-PEE-7 and PE-PEE-17.  $\langle f_{PE} \rangle$  represents the overall volume fraction of PE. These data were acquired while heating the specimens at 0.3 °C/min with a 1% strain amplitude and a frequency of 0.5 rad/s. Order-order phase transitions are associated with a rapid increase or decrease in  $G'$ . Order-disorder transitions are identified by the open triangles. Data have been shifted vertically as noted by the composition labels.

deducing the associated morphology. Although only limited SAXS data are presented in this report, the basis for establishing ordered phases followed the procedures established in numerous previous publications [3-6].

## Results and Analysis

**Phase Behaviour** Phase transition temperatures were identified in nine PE-PEE binary blends ( $0.62 \leq f_{PE} \leq 0.70$ ), formed by mixing PE-PEE-7 and PE-PEE-17 (see Table 1), using isochronal ( $\omega = 0.5$  rad/s)  $G'$  measurements while heating the specimens at 0.3 °C/min. DMS results are presented in Figures 2 (heating) and 3 (heating and cooling). Order-order phase transitions are associated with a rapid increase or decrease in  $G'$ , reflecting differences in the elastic characteristics of specific morphologies [3]. One of the four microstructures shown in Figure 1 is identified with each viscoelastic portion of the  $G'(T)$  curves. These assignments were made using well-

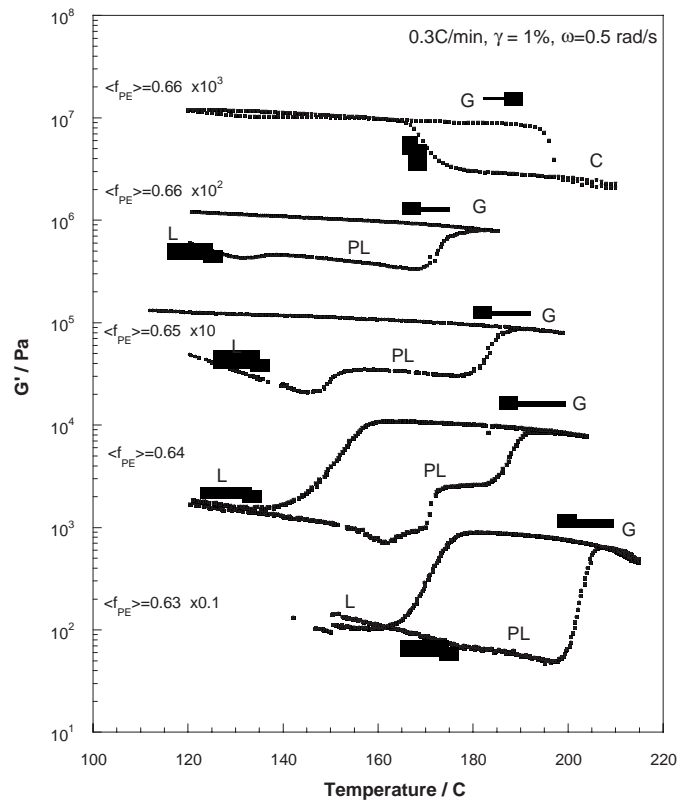


**Figure 3:** Phase behaviour of ordered PE-PEE binary mixtures as a function of heating and cooling under the same conditions as in Figure 2. Two sets of data were recorded for the  $\langle f_{PE} \rangle = 0.66$  specimen: first heating from 120 to 185 °C followed by cooling to 120 °C (lower set), then heating to 210 °C and subsequently cooling to 120 °C (upper set).

established interpretations of SAXS patterns, supported by several TEM micrographs (not shown here). For example, the L phase produces SAXS patterns with reflections at scattering wavevectors  $q^*$ ,  $2q^*$ ,  $3q^*$ , ... where  $q = 4\pi\lambda^{-1}\sin(\theta/2)$  with  $q^* = 2\pi/d^*$ ,  $d^*$  being the lamellae period. A representative SAXS pattern obtained from a lamellae specimen is given in Figure 4a. Upon heating into the PL regime, the second-order reflection disappears as shown in Figure 4b. (Extensive experimentation with this phase in several other block copolymers, including *in-situ* neutron scattering while shearing [18], forms the basis for the phase assignments presented here). The G and C morphologies produce distinctly different SAXS data, with reflections at  $\sqrt{3}q^*$ ,  $\sqrt{4}q^*$ , ... and  $q^*$ ,  $\sqrt{3}q^*$ ,  $\sqrt{4}q^*$ ,  $\sqrt{7}q^*$ , ..., respectively. We have not presented this evidence here since it duplicates comparable results reported in several earlier publications.

Order-disorder transition temperatures ( $T_{ODT}$ ) are signalled by a complete loss of elastic modulus as

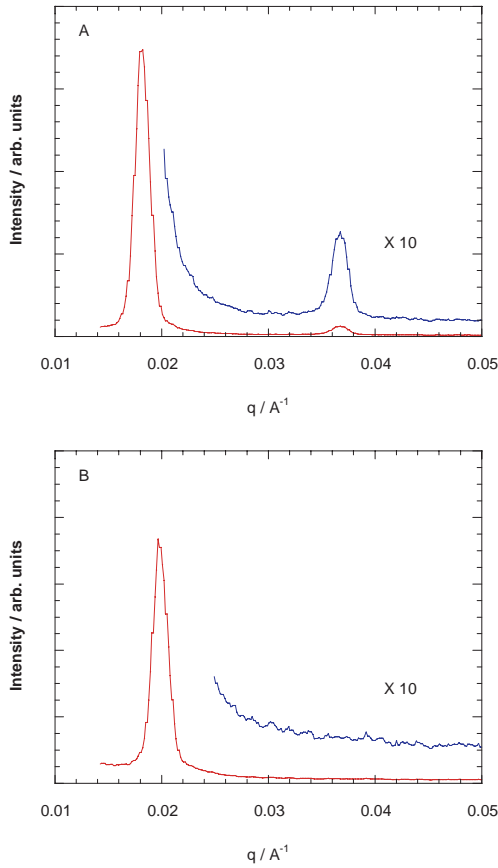


**Figure 4:** Representative SAXS patterns taken from the  $\langle f_{PE} \rangle = 0.63$  mixture. (A)  $T = 160^\circ\text{C}$ . Reflections at relative positions of  $q^*$ ,  $2q^*$ ,... are consistent with a lamella phase. (B) Loss of higher order reflections at  $200^\circ\text{C}$  is associated with the perforated layers phase. Phase assignments are also supported by TEM images (not shown here).

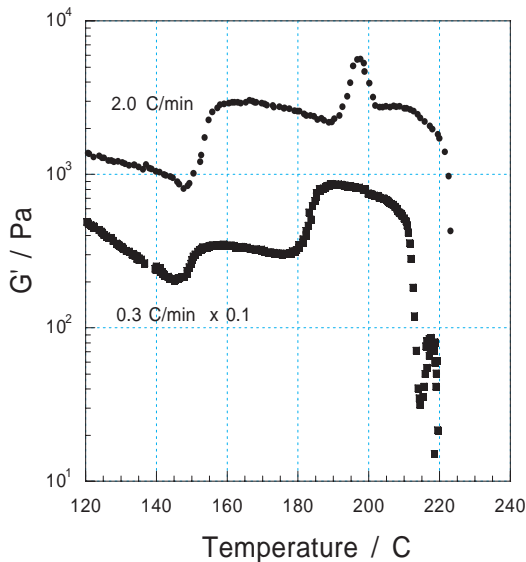


**Figure 5:** Influence of heating rate on  $G'(T)$  for  $\langle f_{PE} \rangle = 0.65$  PE-PEE mixture. Varying the heating rate from  $0.3^\circ\text{C}/\text{min}$  to  $2.0^\circ\text{C}/\text{min}$  switched the transition path from  $\text{PL} \rightarrow \text{G}$  to  $\text{PL} \rightarrow \text{C}$ , respectively. Strain amplitude and frequency are as given in Figure 2.

noted by the open triangles in Figure 2.

A clear pattern of phase behaviour emerges from the  $G'(T)$  results in Figure 2. As  $\langle f_{PE} \rangle$  increases from 0.62 to 0.70 at constant temperature (ca  $180^\circ\text{C}$ ), there is a progression from L to PL to G and finally C. The OOT's form smooth curves as a function of composition and temperature across multiple specimens, carving out well-defined regions for each morphology. For example, the cylindrical state first emerges on heating in the  $\langle f_{PE} \rangle = 0.65$  specimen within  $5^\circ\text{C}$  of  $T_{\text{ODT}}$ . As  $\langle f_{PE} \rangle$  increases the C window broadens, ultimately encompassing the entire experimental temperature range at  $\langle f_{PE} \rangle = 0.69$ . However, all these OOT temperatures are subject to the effects of superheating as illustrated by the results found in Figure 3.

Finite nucleation and growth kinetics result in a delay in the transformation from one ordered state to another. This translates into hysteresis when the material is heated and cooled at a finite rate. These DMS data confirm that upon heating  $\text{L} \rightarrow \text{PL} \rightarrow \text{G}$  while on cooling  $\text{G} \rightarrow \text{L}$ , bypassing the PL phase. This pattern is identical to one documented in PEO-PEE [19] at just one-twentieth the molecular weight of the PE-PEE diblocks. Two different classes of OOT's were probed in the  $\langle f_{PE} \rangle = 0.66$  sample, which exhibits all four morphologies included in Figure 1. At lower temperatures the  $\text{L} \rightarrow \text{PL} \rightarrow \text{G}$  sequence occurs, a natural progression from the behavior at lower compositions (see Figure 2). However, cooling the G phase fails to generate lamellae, a result anticipated by the reduction in  $T_{\text{L}} \rightarrow \text{PL}$  as  $\langle f_{PE} \rangle$  increases; this effect also was encountered in the PEO-PEE study [19]. This is consistent with our hypothesis that PL is a metastable structure that only forms as a long-lived transient state during transformation of lamellae to gyroid. In contrast the higher temperature OOT, is a reversible,  $\text{G} \rightarrow \text{C}$  and  $\text{C} \rightarrow \text{G}$ , albeit hysteretic transition.

*Rate Dependence* We have further probed the dynamics of these phase transitions by varying the rate of heating the  $\langle f_{PE} \rangle = 0.65$  sample while monitoring  $G'$  (Figure 5). Increasing  $dT/dt$  from  $0.3$  to  $2.0^\circ\text{C}/\text{min}$  has little impact on the  $\text{L} \rightarrow \text{PL}$  transition, presumably due to the similarity in symmetry, i.e. both are layered morphologies. However, whereas the sequence  $\text{L} \rightarrow \text{PL} \rightarrow \text{G} \rightarrow (\text{C}) \rightarrow \text{disorder}$  occurs at the lower heating rates, we believe the G phase is bypassed at  $2.0^\circ\text{C}/\text{min}$ , i.e. L

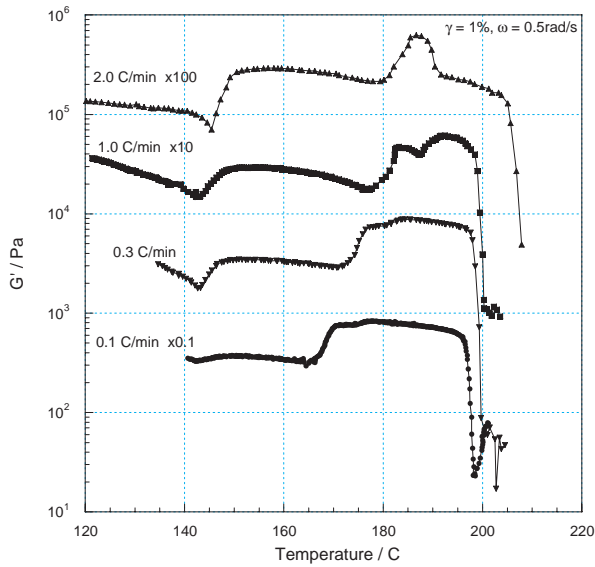


**Figure 6:** Influence of heating rate on  $G'(T)$  for PE-PEE-6, a nearly monodisperse sample. These results are nearly identical to those in Figure 5 confirming that the heating rate dependence of these OOT's is not attributable to mixing.

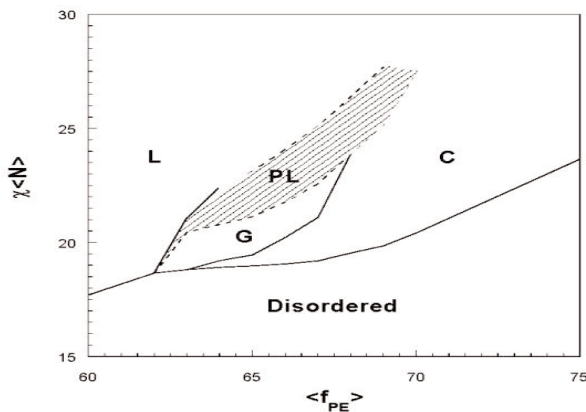


**Figure 7:** Phase portrait of PE-PEE diblock copolymers as a function of the product  $\chi N$  and the composition  $\langle f_{PE} \rangle$ . Phase boundaries have been assigned based on the transition temperatures identified in Figure 2. The PL phase is metastable while L, G, and C are equilibrium states. At equilibrium the indicated order-order phase boundaries will shift up slightly, and the G phase will cover the area denoted PL.

→ PL → C → disorder. We base this deduction on the magnitude of  $G'$  between 190 and 205 °C and the elevated value of  $T_{ODT} = 206$  °C relative to the precipitous drop in  $G'$  at about 195 °C when  $dT/dt = 0.1$  °C/min (also compare these results with those in Figure 2). Apparently there is insufficient time to nucleate the PL → G transition at the higher heating rate. Instead the superheated PL phase forms

cylinders, presumably due to a lower kinetic barrier. We interpret the peak in  $G'(T)$  at about 187 °C as resulting from a transition state structure. Identification of the morphologies underlying these  $G'(T)$  patterns rectifies earlier confusion in making phase assignments to PEP-PEE block copolymers near the ODT.

We have excluded the possibility that the results presented in Figure 5 are influenced by the bimodal composition distribution of the PE-PEE-7/ PE-PEE-17 mixture by repeating the experiments on sample PE-PEE-6, a relatively monodisperse diblock copolymer with the same composition (Table 1).  $G'(T)$  for four representative heating rates (0.1, 0.3, 1.0 and 2.0 °C/min) are presented in Figure 6. Nearly identical phase transitions as those seen in Figure 5 were produced by this compound.

## Discussion

The experiments reported here, together with our earlier studies, allow us to present a complete picture of the network of morphologies and kinetic pathways that govern the phase behaviour of diblock copolymers near the order-disorder transition. Figure 1 includes arrows identifying the known OOT's linking the three equilibrium and one metastable phases that occur near  $f_{PE} = \langle 0.65 \rangle$  in PE-PEE. Upon heating L transforms to PL; this is a thermally reversible transition as shown elsewhere (see Figure 14 in ref. 18). Slowly heating the PL phase results in a transition to G, while rapid heating produces C, both irreversibly. G and C transform reversibly, through an OOT that is known to be mediated by an epitaxial relationship [12]. Cooling G leads to a direct conversion to L, bypassing the metastable PL phase.

We present a phase portrait summarizing our results in Figure 7. Based on  $\chi(T) = 15.0T^{-1} - 0.0055$  [16],  $\chi \langle N \rangle$  is plotted versus  $\langle f_{PE} \rangle$  where  $\langle N \rangle$  is the number average degree of polymerization assuming 4-carbon repeat units. The phase boundaries have been located according to the transition temperatures extracted from Figure 2; due to hysteresis effects these are all displaced to slightly lower  $\chi \langle N \rangle$  than the true equilibrium values. Shading in the PL window signifies metastability. At equilibrium the G phase extends over the entire PL region and the L - G phase boundary lies somewhat higher in  $\chi \langle N \rangle$  than the L - PL boundary (see Figure 7). This phase portrait is strikingly similar to those characterizing

PS-PI, PEP-PEE, PEP-PDMS, and PEO-PEE.

One notable exception to this universal picture is the PE-PEP system in which the G phase has never been identified [2, 20]. Based on the results reported here we can finally understand this puzzling disparity. PE and PEP are nearly compatible, requiring a molecular weight of more than  $10^5$  g/mol to induce microphase separation at 150 °C [16]. Also, PE and PEP both are characterized by low entanglement molecular weights ( $M_{e,PE} \approx 1,000$  and  $M_{e,PEP} \approx 1,600$  g/mol compared with  $M_{e,PEE} \approx 10,000$  g/mol [21]). Taken together these two facts lead to extremely slow single chain dynamics in microphase separated PE-PEP relative to the other systems listed above. Thus, the commonly applied heating protocol of 1-2 °C/min while probing OOT's will access the "fast heating" branch in Figure 1, and therefore the PL  $\rightarrow$  C transition in PE-PEP. Thus, it would be difficult to access the G phase in PE-PEP (the most entangled and highest molecular weight diblocks studied [2]), in a steady heating experiment, since switching to the "slow" heating branch will require an unfeasible reduction in heating rate of orders of magnitude.

Decreasing the molecular weight of the block copolymer (this requires an increase in incompatibility if  $\chi N$  is to remain constant) and increasing  $M_e$  ultimately leads to a crossover from a single chain dynamic limit (which dominates the PE-PEP system) to a regime governed by nucleation and growth. Apparently the PE-PEE system lies near this crossover since both the "slow" (PL  $\rightarrow$  G) and "fast" (PL  $\rightarrow$  C) heating branches are accessible (Figures 5 and 6). All available evidence suggests that lower molecular weight, and less entangled, systems (e.g. PS-PI [4], PS-PVP [5], PEP-PDMS [22], PEO-PEE [19]) follow "fast" branch kinetics (i.e. the PL  $\rightarrow$  G transition), consistent with dynamics dictated by nucleation and growth. In fact, the consequences of these effects may be evident within the PE-PEE (and PEP-PEE) system itself. The complex phase window centered around  $\langle f_{PE} \rangle = 0.40$  does not exhibit the heating rate dependence evident in Figures 5 and 6; e.g., the G phase appears at  $dT/dt = 2.0$  °C/min [2]. We believe this is a consequence of the higher percentage of PEE, hence a significantly higher average entanglement molecular weight, in these specimens.

## Summary

Dynamic mechanical spectroscopy and small-angle X-ray scattering experiments with binary mixtures of PE-PEE diblock copolymers over the composition range  $0.60 \leq \langle f_{PE} \rangle \leq 0.75$  have resulted in a complete network of phase transitions between the equilibrium (L, G, and C) and metastable (PL) phases. Phase transition pathways were shown to be strongly influenced by both single chain dynamics and nucleation and growth rates. These results clarify the occurrence of the PL phase and absence of G in certain high molecular weights systems.

## Acknowledgments

Partial support for this work was provided by Showa Denko K.K. (HT) and by the Materials Research Science and Engineering Center (MRSEC) at the University of Minnesota.

## References

- [1] Almdal, K., Koppi, K.A., Bates, F.S. and Mortensen, K., *Macromolecules* (1992) 25, 1743.
- [2] Bates, F.S., Schultz, M.F., Khandpur, A.K. et al., *Faraday Discuss.* (1994) 98, 7.
- [3] Zhao, J., Majumdar, B., Schultz, M.F. et al., *Macromolecules* (1996) 29, 1204.
- [4] Khandpur, A.K., Förster, S., Bates, F.S. et al., *Macromolecules* (1995) 28, 8796.
- [5] Schulz, M.F., Khandpur, A.K., Bates, F.S. et al., *Macromolecules* (1996) 29, 2857.
- [6] Hajduk, D.A., Takenouchi, H., Hillmyer, M.A. et al., *Macromolecules* (1997), 30, 3788.
- [7] Matsen, M.W. and Bates, F.S. *Macromolecules* (1996) 29, 1091.
- [8] Chung, C.I. and Gale, J.C. *J. Polym. Sci., Polym. Phys. Ed.* (1976) 14, 1149.
- [9] Gouinlock, E.V. and Porter, R.S. *Polym. Eng. Sci.* (1977) 17, 535.
- [10] Han, C.D., Kim, J. and Kim, J.K. *Macromolecules* (1989) 22, 383.
- [11] Rosedale, J.H. and Bates, F.S. *Macromolecules* (1990) 23, 2329.
- [12] Schulz, M.F., Bates, F.S., Almdal, K. et al., *Phys. Rev. Lett.* (1994) 73, 86.
- [13] Matsen, M.W. and Bates, F.S. *Macromolecules* (1996) 29, 7641.
- [14] Qi, S. and Wang, Z.-G., *Phys. Rev. Lett.* (1996) 76, 1679.

- [15] Shi, A.-C., Desai, R.C. and Noolandi, J.  
*Phys. Rev. Lett.* (1997) 78, 2577.
- [16] Rosedale, J.H., Bates, F.S., Almdal, K. et al., *Macromolecules* (1995) 28, 1429.
- [17] Bates, F.S., Rosedale, J.H., Bair, H.E., et al., *Macromolecules* (1989) 22, 2557.
- [18] Hamley, I.W., Gehlsen, M.D., Khandpur, A.K. et al., *J. Phys. II*, France (1994) 4, 2161.
- [19] Hillmyer, M.A., Bates, F.S., Almdal, K. et al., *Science* (1996) 271, 976.
- [20] Rosedale, J.H., PhD Thesis, University of Minnesota (1993).
- [21] Fetters, L.J., Lohse, D.J., Richter, D. et al., *Macromolecules* (1994) 27, 4639.
- [22] Vigild, M.E., Almdal, K., Mortensen, K. et al., *Macromolecules* (1998) 31, 5702.

## Modelling diffraction patterns from a textured polycrystalline sample

Y. Nishiyama<sup>1</sup> and P. Langan<sup>2</sup>

1. Graduate School of Agricultural and Life Science,  
University of Tokyo, Yayoi, Tokyo 113-8657, Japan

2. B. Division, Los Alamos National Laboratory, MS-M888,  
Los Alamos NM87545 USA

### Introduction

Fibre diffraction studies have enabled structural information to be extracted from materials that are difficult to crystallize into macroscopic single crystals or when the state of interest is not highly crystalline. It is usually assumed that the sample is an aggregate of basic scattering units, each with an associated unique axis. The scattering units either exhibit rotational symmetry about the unique axis or the distribution of orientations about the unique axis is random. In addition to this, the distribution of the unique axis itself is given by a function that has rotational symmetry about a preferred direction, called the fibre axis. This is a good approximation for fibrous materials with diffraction information uniformly distributed around the fibre axis. However, there are fibrous, polycrystalline materials in which the distribution of the unique axis does not have rotational symmetry about the fibre axis or in which the scattering units are not uniformly orientated around the unique axis. The first effect is often referred to as texture. When the second effect corresponds to a second direction in the basic scattering unit being preferentially oriented around a second axis in the fibre it is referred to as biaxial orientation. In our studies of the crystal structure of native cellulose we have obtained sharp diffraction data extending to 1Å resolution (1) but exhibiting complex texture resulting from a combination of the two effects mentioned above. This problem also afflicts quasi-single-crystalline  $\alpha$ -chitin from which good data have been collected recently (2), but the refined structure has yet to emerge due to the lack of proper software to deal with diffraction data from a specimen of complex texture. This article describes a realistic approach to processing diffraction data from fibre specimens with complex texture and is illustrated with the structure of native cellulose as an example.